Highly Potent Cationic Chitosan Derivatives Coupled to Antimicrobial Peptide Dendrimers to Combat *Pseudomonas Aeruginosa*

*Olivier Jordan, Bee-Ha Gan, Sari Alwan, Karl Perron, Emmanuelle Sublet, Verena Ducret, Hua Ye, Gerrit Borchard, Jean-Louis Reymond and Viorica Patrulea**

O. Jordan, S. Alwan, K. Perron, E. Sublet, G. Borchard, V. Patrulea

Institute of Pharmaceutical Sciences of Western Switzerland, University of Geneva

1 Rue Michel Servet, 1211 Geneva, Switzerland

O. Jordan, S. Alwan, K. Perron, E. Sublet, G. Borchard, V. Patrulea

Section of Pharmaceutical Sciences, University of Geneva

1 Rue Michel Servet, 1211 Geneva, Switzerland

B.-H. Gan, J.-L. Reymond

Department of Chemistry and Biochemistry, University of Bern

Freiestrasse 3, 3012 Bern, Switzerland

K. Perron, V. Ducret

Microbiology Unit, Department of Botany and Plant Biology, University of Geneva

This article has been accepted for publication and undergone full peer review but has not been through the copyediting, typesetting, pagination and proofreading process, which may lead to differences between this version and the Version of Record. Please cite this article as doi: 10.1002/adhm.202304118.

30, Quai Ernest-Ansermet, 1211Geneva, Switzerland

H. Ye, V. Patrulea

Institute of Biomedical Engineering, Department of Engineering Science, University of Oxford

Oxford, OX3 7DQ, UK

E-mail: viorica.patrulea@unige.ch

Keywords: Chitosan derivatives, antimicrobial agents, antimicrobial peptide dendrimers (AMPDs), antimicrobial peptides (AMPs), Gram-negative *P. aeruginosa*

The burden of bacterial wound infections has considerably increased due to antibiotic resistance to most of the currently available antimicrobial drugs. Herein, we report for the first time a chemical coupling of two cationic *N*-aryl (pyridyl and aminocinnamyl) chitosan derivatives to antimicrobial peptide dendrimers (AMPDs) of different generations (first, second and third) *via* thioether-haloacetyl reaction. The new chitosan-AMPD conjugates showed high selectivity by killing *Pseudomonas aeruginosa* and very low toxicity towards mammalian cells, as well as extremely low hemolysis to red blood cells. Electron microscopy revealed that the new chitosan derivatives coupled to AMPD destroyed both the inner and outer membranes of Gram-negative *P. aeruginosa*. Moreover, chitosan-AMPD conjugates showed synergetic effects within extremely low concentrations. The new chitosan-AMPD conjugates can be used as potent antimicrobial therapeutic agents, to eradicate pathogens such as those present in acute and chronic infected wounds.

Introduction

Antimicrobial resistance (AMR) has become one of the major global threats despite significant efforts to find appropriate antimicrobial agents. Antibiotic-resistant bacteria lead to 700,000 deaths annually and at least 35,900 deaths in the United States alone.[1, 2] By 2050, AMR could be the leading cause of death, with an estimated 10 million annual deaths. As such, it is imperative that rapid actions are taken to find solutions to combat AMR bacteria.[3, 4] *Pseudomonas aeruginosa* is one of the most relevant opportunistic pathogens[5] that belong to the ESKAPE family (*Enterococcus faecium*, *Staphylococcus aureus*, *Klebsiella pneumoniae*, *Acinetobacter baumannii*, *Pseudomonas aeruginosa*, and *Enterobacter spp.*) [6, 7]. Their multidrug resistance to most antibiotics makes them one of the most serious threats, causing nosocomial infections and chronic infections in cystic fibrosis.[8] Currently, there are extremely limited options to combat *P. aeruginosa*, relying mainly on antipseudomonal carbapenems, cephalosporins, aminoglycosides, and fluoroquinolones.[9, 10] Polymyxin B can be used to treat *P. aeruginosa* infections, but this should be used only as a last resort because of the high incidence of neuro- and nephrotoxicity.[11, 12] Previous reports on biopolymers, such as chitosan, have shown potency to reduce biofilm,[13, 14] although chitosan antimicrobial activity requires acidic conditions. Chitosan derivatives, such as quaternized ones, may be effective in eradicating *P. aeruginosa,*[15] although at high doses. Novel derivatives have also shown low toxicity to human cells.[16] Still, given therapeutic applications, effective compounds require high activity and low toxicity toward red blood cells, *i.e.,* low hemolysis rates. We hypothesized that conjugation with novel antimicrobial peptides could produce biopolymer derivatives of clinical interest.

Antimicrobial peptides (AMPs) have gained significant attention for their clinical potential as a new class of antibiotics in eradicating both Gram-negative and Gram-positive pathogens. AMPs have shown high and broad antibacterial properties against different pathogens, including multidrug-resistant (MDR) bacteria.[17] Antimicrobial peptide dendrimers (AMPDs) have recently emerged as new potential candidates in combatting Gram-negative bacteria. They have a three-dimensional branched structure with very dense and flexible functional groups.[18] Studies from Reymond's group have previously reported that AMPDs had remarkable activity against Gram-negative *P. aeruginosa*, *A. baumannii, and E. coli.*[19] G3KL, a third-generation AMPD has selective properties that disrupt the

bacterial membrane[20] while exhibiting pro-angiogenic properties, leading to endothelial tubular network formation.[21] Additionally, it has been shown to effectively kill MDR *A. baumannii* and *P. aeruginosa*, as well as to confer antibiofilm properties with a low propensity for resistance development.[22] Furthermore, it was recently shown that after disrupting bacterial membrane, AMPDs interact with DNA and accumulate in Gram-negative bacteria, leading to vesicle leakage, and cell death.[23] However, their clinical use is hindered due to reported toxicity, hemolysis towards mammalian cells, and fast proteolytic degradation.[24] These shortcomings could be addressed by covalently coupling AMP(D)s and chitosan derivatives to induce synergistic antibacterial activities and very low toxicity.

Recently, we demonstrated that chitosan linked to peptide dendrimers displayed remarkable synergy and effectively killed Gram-negative bacteria pathogens.[24] Specifically, we conjugated AMPs to CM-TMC (*3,6-di-O*-carboxymethyl-*N,N,N*-trimethyl chitosan) and CMC (*3,6-di-O*-carboxymethyl chitosan), which showed synergistic activity between chitosan and AMPDs.[24]

Such conjugates should ideally optimize the balance ratio between antimicrobial potency and hemolytic activity so that a broad range of doses can be safely administered – the so-called therapeutic window. Previously published derivatives still show some toxicity towards dermal fibroblasts at high doses, therefore one of the goals of the present study was to provide novel and more effective derivatives with improved therapeutic window, by limiting toxicity towards healthy mammalian cells.[24]

To demonstrate the platform's versatility and further improve the efficacy and non-toxicity of the conjugates, we focused on developing new AMPD-chitosan derivatives. Thus, we covalently coupled G3KL to CM-TM-PMC (*3,6*-di-*O*-carboxymethyl-*N*-4-*N,N,N*-trimethyl-aminocinnamyl chitosan) and CM-TM-DMAC (*3,6*-di-*O*-carboxymethyl-*N*-4-*N,N,N*-trimethyl-pyridylmethyl chitosan). The antimicrobial activity of chitosan-AMPD conjugates was tested against *P. aeruginosa*, and the safety profile was checked against mammalian cells and red blood cells. Transmission electron microscopy (TEM) and scanning electron microscopy (SEM) imaging were used to check the mechanism of killing. Moreover, the coupling efficiency of this new chitosan-based technological platform was tested on the second and third-generation AMPD, G2KL, and G3KL, respectively, as well as a linear AMP, such

as SB1. This study aims to prove the versatility of the chitosan technology for coupling efficiently not only linear but also branched AMPs.

Results and Discussions

NMR and FTIR for chitosan derivatives synthesized

The synthesis of DAH-CM-TM-PMC and DAH-CM-TM-DMAC was carried out in different steps as shown in Figure 1. The *N*-arylation of *N*-4-pyridylmethyl chitosan (PMC) and N-(4-*N,N*-dimethylaminocinnamyl) chitosan (DMAC) derivatives were obtained by reductive amination *via* formation of a Schiff base intermediate with sodium cyanoborohydride by reacting primary amino groups of chitosan with aldehydes under homogeneous acidic conditions. The Schiff base was then reduced with sodium cyanoborohydride. *N*-methylation step was carried out using methyl iodide and sodium iodide in excess in the presence of sodium hydroxide to achieve quaternization or *N,N*-dimethylaminocinnamyl, or *N*-pyridylmethyl or primary amino groups of chitosan. The methylation reaction is based on the nucleophilic substitution of primary amine from C-2 with methyl groups with their counter-ions, which were further exchanged with chlorine for stability reasons. The final quaternized chitosan derivatives were positively charged and water-soluble at neutral pH. Introducing permanent positive moieties helps antimicrobial activities to chitosan derivatives, as shown by other groups.[16]

The successful synthesis of the chitosan derivatives has been confirmed by both NMR and FTIR. Chemical shifts for *N*-aryl derivatives were attributed according to the literature.[16, 25, 26] The degree of *N*-substitution (DS_{Ar}), degree of trimethylation of N-aryl units ($DS_{TM\ Ar}$), degree of trimethylation of GlcN units (DS_{TM}), degree of carboxymethylation (DS_{CM}) was calculated using Equations 1 – 4 and reported in Table 1 (more details in Table S1).

$$DS_{\mathrm{Ar}} = \frac{[Ar]}{n} \times \frac{1}{\left([H_2]+\frac{1}{3}[NHAc]\right)} \quad (1)$$

where, $[Ar]$ represents the integral area between 7 – 9 ppm, corresponding to aromatic protons, n is number of aromatic hydrogens, $[H_2]$ is for integral area for GlcN residues, while [NHAc] is for GlcNAc residues from chitosan backbone.

$$DS_{TM} = \frac{[N^+(CH_3)_3]}{9} \times \frac{1}{[H_1]} \quad (2)$$

where, $[N^+(CH_3)_3]$ represents the integral area corresponding to *N,N,N*-trimethyl groups at 3.2 ppm, $[H_1]$ is number of protons corresponding to H_1 and H_1'.

$$DS_{TM_{Ar}} = \frac{[Ar\ N^+(CH_3)_3]}{9} \times \frac{1}{[H_1]} \quad (3)$$

where, $[Ar\ N^+(CH_3)_3]$ represents the integral area corresponding to *N,N,N*-trimethyl groups from *N*-aryl derivative at 3.5 ppm.

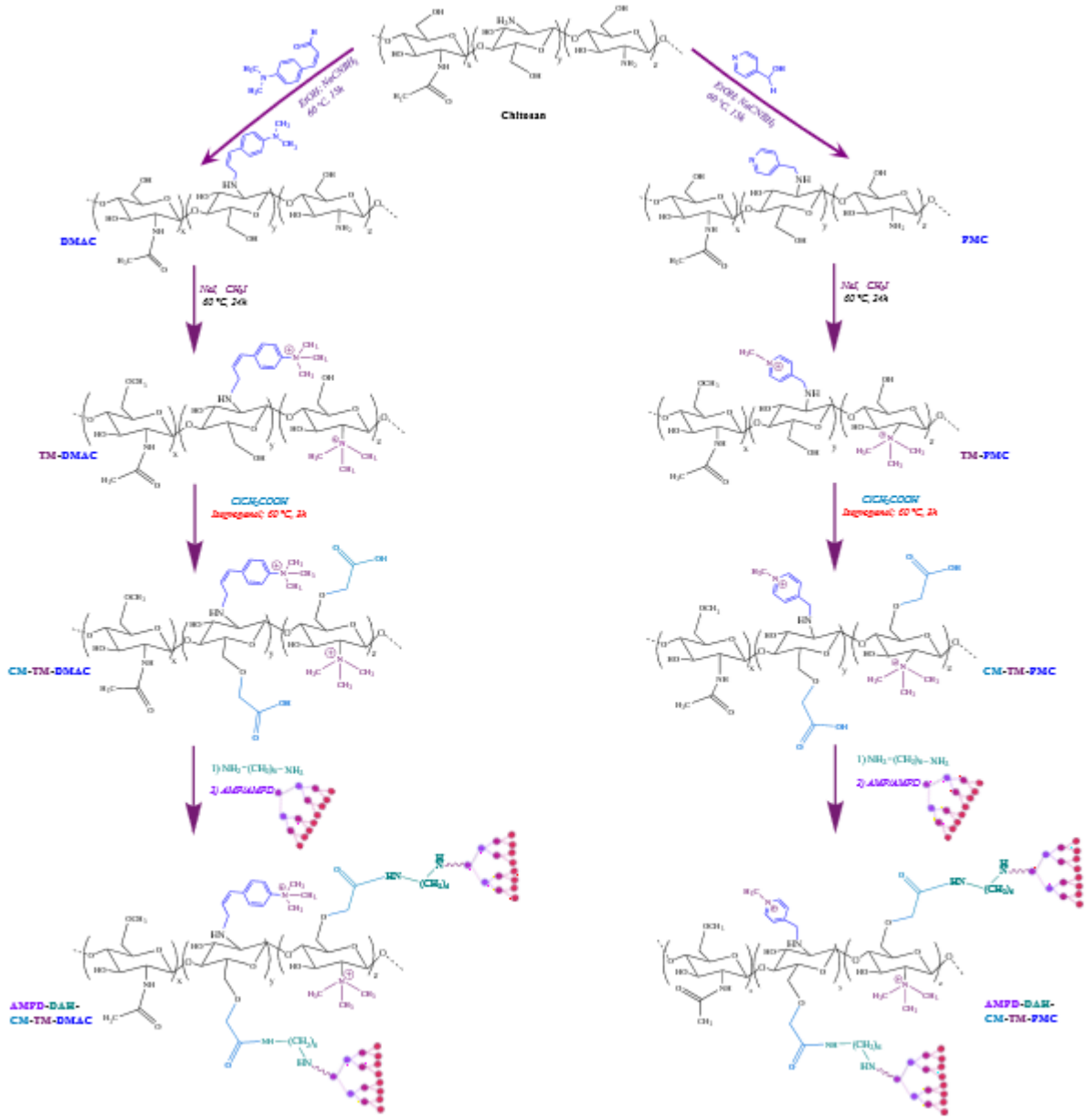

Figure 1. Schematic representation for the synthesis of the final products.

Carboxymethylation of positively charged TM-PMC or TM-DMAC was performed by adding an excess of chloroacetate[27] and the DS was calculated as mentioned in Equation 4:

$$CM = \frac{[-CH_2-COO]}{2} \times \frac{1}{[H_1]} \quad (4)$$

where, $[-CH_2 - COO]$ represents the integral area corresponding to *O*-carboxymethyl groups present on H3 and H6 from 4 - 4.25 ppm.

DAH spacer addition allows better flexibility of the AMPD, decreasing steric hindrance and potentially improving interaction with the bacterial wall.[27]

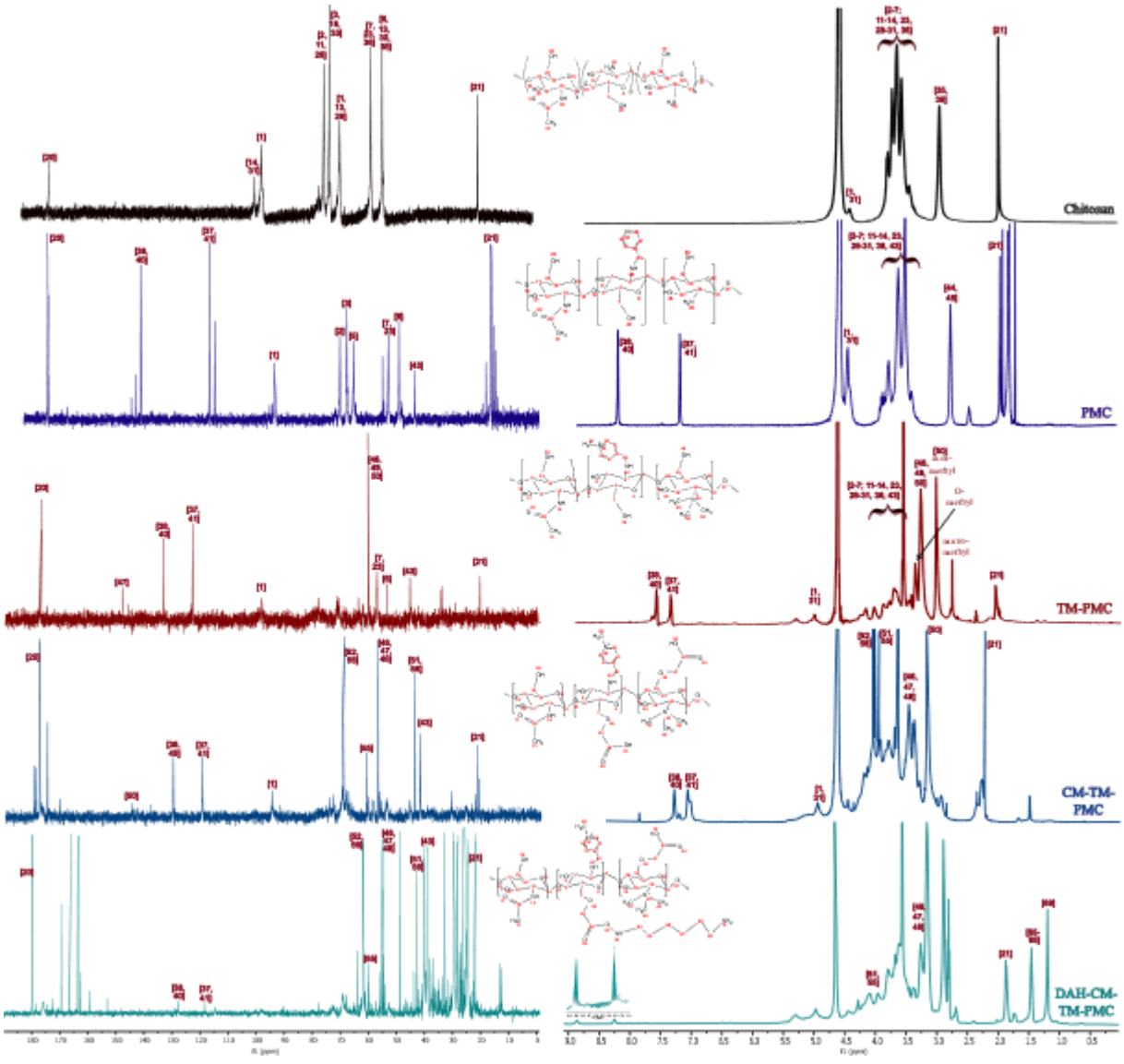

Figure 2. The ^{13}C (left) and ^{1}H (right) NMR spectra of pyridyl chitosan derivatives in D_2O recorded at 298 K starting from raw chitosan to DAH-CM-TM-PMC.

NMR spectra (Figure 2 and Figure S1-S8) confirm the achievement of each step of the synthesis. ^{1}H-NMR for **chitosan**: δ (ppm) = 2.0 (3H, $NHCOCH_3$), 3.1 (2H, NHGlcN), 3.52-4.05 (22H, H2-H6); for **PMC:** 8.43, 7.38 (2 x 2H, Ar); for **TM-PMC:** 7.75, 7.46 (2 x 2H, Ar), 3.4 (3 x 3H, $N^+(CH_3)_3$), 3.6-4.1 (1 x 3H, $N(CH_3)$, Ar; 7H, CH_2-NH, H3-H6), 3.02 (6H, $N(CH_3)_2$), 2.76, (1 x 3H, $N(CH_3)$; for **CM-TM-PMC:** 4.02-4.15 (2H, CH_2); for **DAH-CM-TM-PMC**: 1.26 (2H, CH_2NH2), 1.47 (4 x 2H, CH_2); for **G1-DAH-CM-TM-PMC:** 1.26, 2.13 and 2.44 (lysine and leucine); for **G2-DAH-CM-TM-PMC:** 2.13 and 2.43 (for lysine and leucine); for **G3-DAH-CM-TM-PMC**: 1.25, 2.06 and 2.35 ppm, and ^{13}C-NMR for **chitosan**: δ (ppm) = 22.1 ($COCH_3$), 71.14 ($NHCH_2$), 56.0, 60.4, 74.8, 101.3 (C13 and C38; C7, C23 and C36; C3 and C33; C1); for **PMC:** 124.0, 148.3 (C-Ar), 50.0 (C43); for **TM-PMC:** 123.7, 148.9 (C-Ar), 134.3 (C47), 57.8 ($N^+(CH_3)_3$), 34.8 ($N(CH_3)_2$); for **CM-TM-PMC:** 70.0 (COO), 44.3 (C55, C51); for **DAH-CM-TM-PMC**: 24.5 (C69) and 29.2 ppm (C65-C68); for **G1-DAH-CM-TM-PMC:** 21.26, 26.92 and 28.83; for **G2-DAH-CM-TM-PMC:** 1.27, 2.13 and 2.42, and for **G3-DAH-CM-TM-PMC**: 21.05, 24.58 and 28.64 ppm.

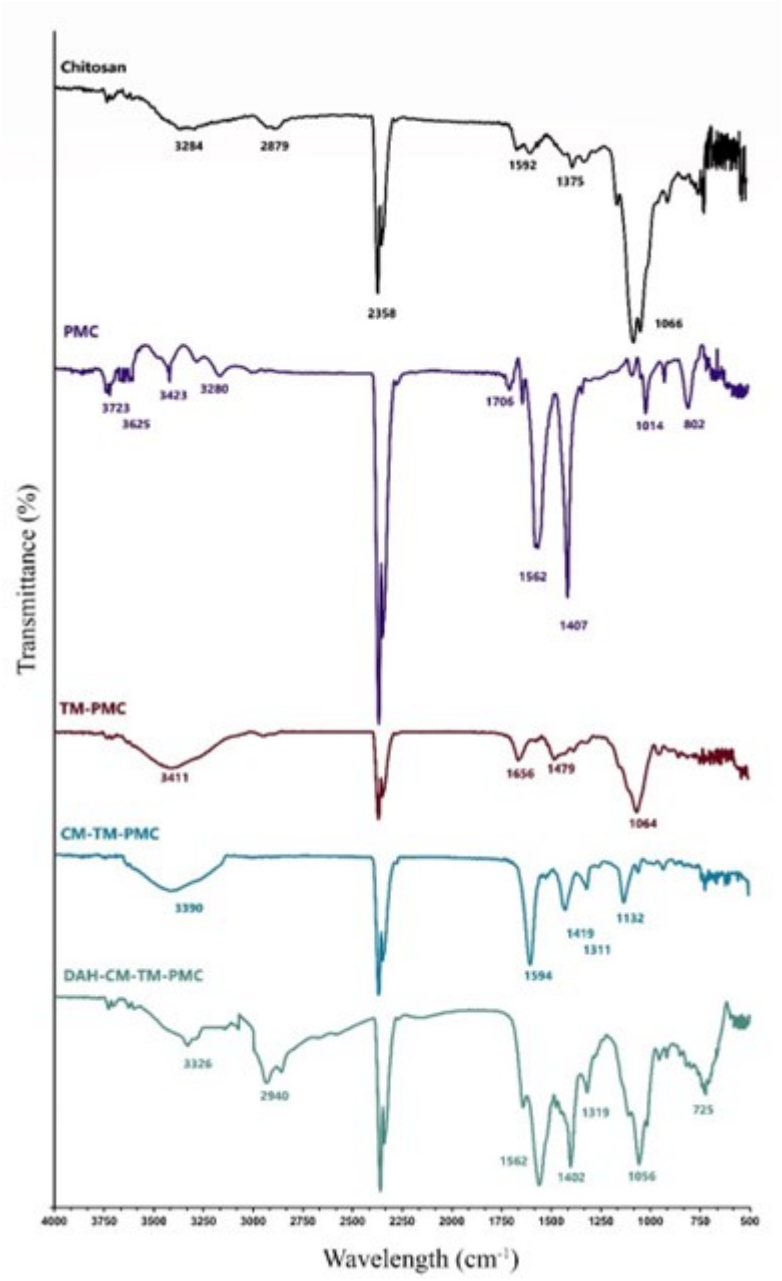

Figure 3. FTIR spectra of pyridyl chitosan derivatives starting from raw chitosan to DAH-CM-TM-PMC.

We observed that the methylation step with sodium iodide followed by the addition of CH_3I reacted slightly differently from one batch to another, thus resulting in low yield for specific reaction steps (Table 1). The degree of substitution for *N*-aryl derivatives was 38%. Moreover, *O*-methylation

during the methylation step was noticed, which would further lead to low yield and higher steric hindrance, and less peptide grafting. *O*-methylation is known to lead to chain scission as well.[26, 28] A low degree of trimethylation would favor peptide grafting and less toxicity. However, balancing non-toxicity versus efficacy should be considered before choosing an appropriate degree of trimethylation. FTIR spectra (Figure 3) confirmed the presence of functional groups present at each step of the reaction. The signals observed in **chitosan** are: at 3284 (N-H and O-H); 2879 (C-H); 1592 and 1375 (C═O, amide groups); 1153 (C–O-C), and 1066 cm^{-1} (C-O); in **PMC:** 3280 cm^{-1} (O-H and N-H, GlcN); 1706, 1637, 1562 and 1407 cm^{-1} (C=C, Ar); and 802 cm^{-1} (C-H, Ar); in **TM-PMC:** the 1656 and 1479 cm^{-1} (C-H, $N^{+}(CH_3)_3$); in **CM-PMC:** 1594 and 1419 cm^{-1} (CH_2-COO); **DAH-CM-TM-PMC**: 2940 cm^{-1} (CH_2); 1562 and 1402 cm^{-1} (N-H-O).

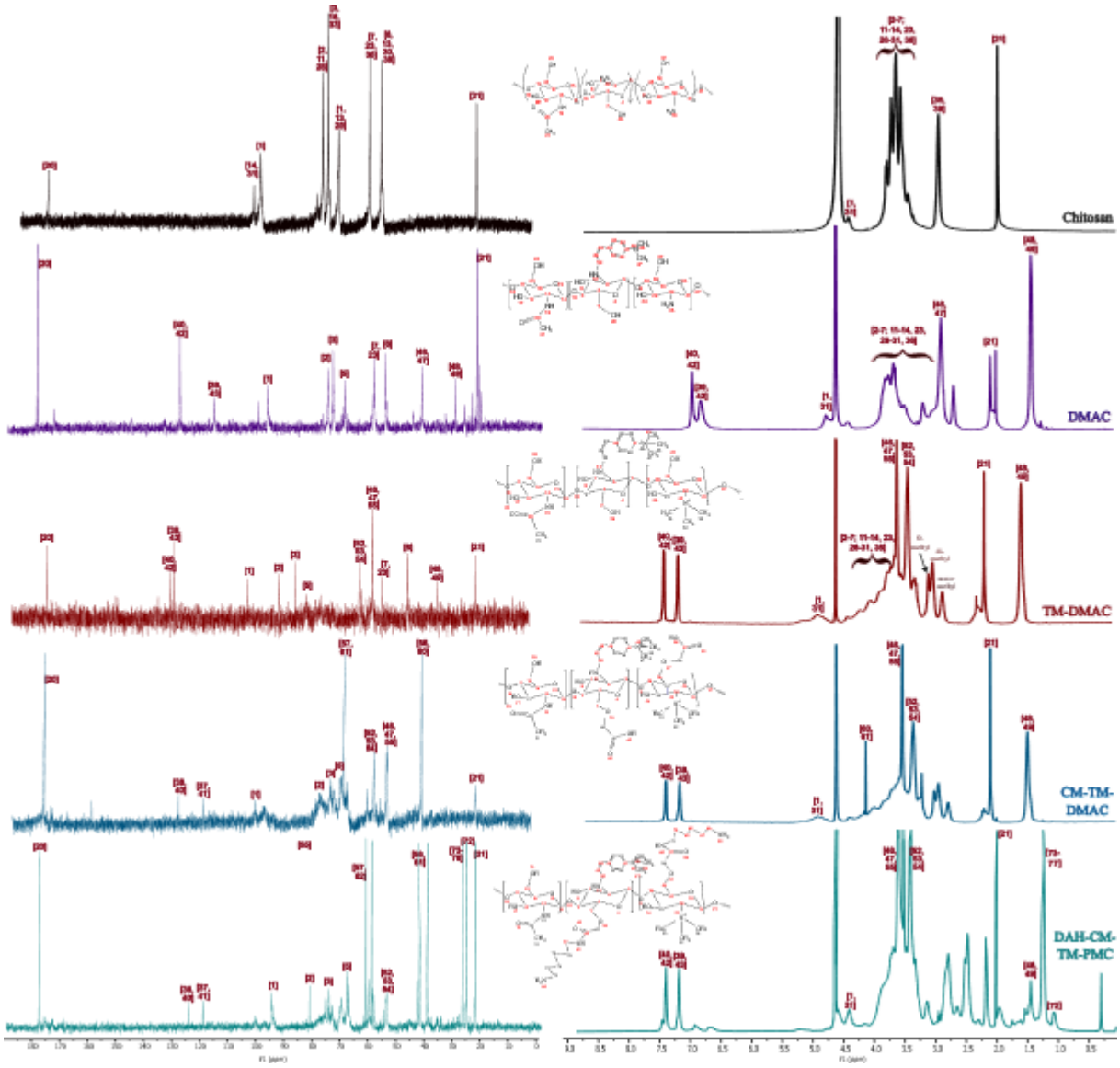

Figure 4. The ^{13}C (left) and ^{1}H (right) NMR spectra of dimethylaminocinnamyl-*N*-aryl chitosan derivatives in D_2O recorded at 298 K starting with chitosan to DAH-CM-TM-DMAC.

In Figure 4 (and Figure S9-S15), the ^{13}C and ^{1}H-NMR spectra confirm successful derivatization. ^{1}H-NMR for **chitosan**: δ (ppm) = 2.0 (3H, $NHCOCH_3$), 3.1 (2H, NHGlcN), 3.52-4.05 (22H, H2-H6); for **DMAC**: 7.11, 7.36 (2 x 2H, Ar), 3.3 (6H, $N(CH_3)_2Ar$), 1.36 (4H, CH_2CHCH); for **TM-DMAC**: 7.54, 7.78 (2 x 2H, Ar), 3.3-4.34 (31H; 7H, CH_2-NH, H2-H6, 2 x 3H, 3,6-*O*-CH_3, 9H, $N(CH_3)$, Ar, $N^+(CH_3)_3$), 2.82 (3H, $NHCH_3$), 3.0 (2 x 3H, $NH(CH_3)_2$); for **CM-TM-DMAC**: 4.05-4.27 (2H, CH_2); for **DAH-CM-TM-DMAC**: 1.1 (2H, CH_2NH_2), 1.3 and 1.4 (4 x 2H, CH_2); for **G1-DAH-CM-TM-DMAC:** 1.24, 2.13 and 2.46 (for lysine and leucine); for **G2-DAH-CM-TM-DMAC:** 1.27, 2.13 and 2.42 (lysine and leucine); for **G3-DAH-CM-TM-DMAC**: 1.24, 2.13 and 2.42 ppm, and ^{13}C-NMR for **chitosan**: δ (ppm) = 22.1 ($COCH_3$), 71.14 ($NHCH_2$), 56.0, 60.4, 74.8, 101.3 (C13 and C38; C7, C23 and C36; C3 and C33; C1); for **DMAC**: 128.7; 116.6 (C-Ar), 42.1 ($N(CH_3)_2$, Ar), 30.1 (C48-C50); for **TM-DMAC**: 131.5; 130.0 (C-Ar); 58.7 ($N^+(CH_3)_3$, 62.8 ($N^+(CH_3)_3$, Ar); for **CM-TM-DMAC**: 69.5 (COO), 41.4 (C56, C60); for **DAH-CM-TM-DMAC**: 24.0 (C72), 26.1 (C73-C76) and 67.5 ppm (C66); for **G1-DAH-CM-TM-DMAC:** 21.46, 26.42 and 28.85; for **G2-DAH-CM-TM-DMAC:** 21.58, 26.46 and 28.9, and for **G3-DAH-CM-TM-DMAC**: 22.33, 26.15 and 28.84 ppm.

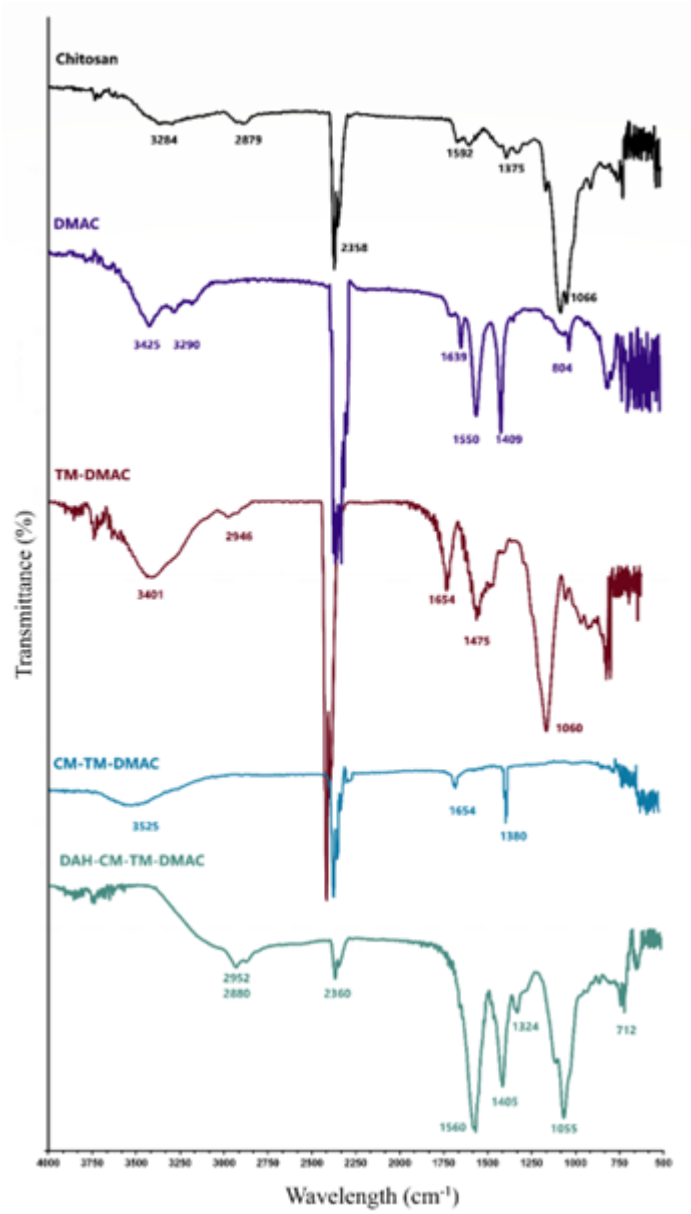

Figure 5. FTIR spectra of dimethylaminocinnamyl-*N*-aryl chitosan derivatives

In Figure 5, FTIR spectra with the following absorption bands are presented. The signals observed in **DMAC** are: 1639, 1550, 1409 (C=C, Ar) and 804 cm^{-1} (C-H, Ar); in **TM-DMAC**: at 1475 cm^{-1} (C–H, Ar), 1654 cm^{-1} ($N^{+}(CH_3)_3$, Ar); **CM-TM-DMAC**: 1654 and 1380 cm^{-1}(CH2COO); **DAH-CM-TM-DMAC**: 2952 cm^{-1} (CH_2), and 1560 cm^{-1} (N-H-O).

Table 1. Results for quantification of the degree of substitution during different steps of synthesis accompanied by their mass yield (%) relative to the starting chitosan mass.

Chitosan Derivatives	DS_{Ar} (%)	$DS_{TM\ Ar}$ (%)	DS_{TM} (%)	DS_{CM} (%)	Stepwise Yield (%)
PMC	38	-	-	-	80
TM-PMC	23		25	-	64
CM-TM-PMC	-	-	-	16	48
DMAC	50	-	-	-	61
TM-DMAC	27	33	25		55
CM-TM-DMAC	-	-	-	22	20

AMPD degree of grafting by amino acid analysis

Previously, we have seen that coupling AMPDs to chitosan derivatives leads to synergistic activities.[24] To improve the activity of the peptide dendrimers or linear peptide, we functionalized G3KL, G2KL, and SB1 peptides by adding one cysteine (cys) at the core of the AMPD and then coupled them to the chitosan derivatives. The coupling reaction *via* thioether-haloacetyl chemistry was performed by reacting the thiol group from the AMP(D) with the primary amine from chitosan derivatives through the addition of a sulfo-SIAB crosslinker. The degree of peptide grafting was analyzed based on the AAA results (Table 2). We could observe that in general, AMPD coupled to pyridyl-conjugates resulted in a lower grafting degree but showed higher antimicrobial activities than for AMPD-cinnamyl-conjugates. A low grafting degree could be attributed to the presence of *O*-methylation in all chitosan derivatives, thus there will be no free space allocated for peptide grafting. Also, mono- and dimethyl units were observed in the NMR spectra alongside the trimethyl moieties. Higher antimicrobial activity is likely due to positive charges confirmed by NMR and FTIR spectra (Figure 2 – 5; Figure S1-S15; Table 1, Table S1). On the other hand, linear AMP showed higher activity when coupled to cinnamyl than pyridyl- conjugates. This difference in activities could be attributed to different steric hindrances, positive charges found in chitosan derivatives, and the ramification degree of the AMPD/AMP (structures detailed in Figure S16-S18). Less steric hindrance would be found in pyridyl-conjugates and therefore higher biological activity was found, thus higher synergy as

well (Table 2). For instance, G3KLcys-CM-TM-DMAC showed no synergy upon coupling, although their chemistry resulted in the highest degree of grafting. We hypothesize that the main factor is the effective presentation of AMP(D) to cells, avoiding loss of AMP(D) activity due to steric hindrance. The fractional inhibitory concentration (FIC) index was calculated according to Equation 5, based on the Chou-Talalay method,[29] which defines synergism (FIC < 1), additive (FIC = 1) and antagonism (FIC > 1) effect.

$$FIC_{index} = FIC_A + FIC_B = \frac{MIC_{combination\ A\&B}}{MIC_{agent\ A}} + \frac{MIC_{combination\ A\&B}}{MIC_{agent\ B}} = \Sigma\ \mathrm{FIC} \quad (5)$$

Table 2. Properties of peptide-chitosan conjugates/chitosan derivatives: grafting degree from amino acid analysis (AAA), mass yield (%), minimal inhibitory concentration (MIC), and synergy level of the antimicrobial effect.

Peptide-chitosan conjugate	Grafting degree (%)	Yield (%)	MIC (µg mL^{-1})	Synergy level
G3KLcys	-		8-16	
G2KLcys	-		128	
SB1cys	-		16	
Chitosan (physiological pH)	-		>TC*	
CM-TMC-PMC	-		>TC*	
G3KLcys-DAH-CM-TM-PMC	10.2	99	3.3	****
G2KLcys-DAH-CM-TM-PMC	10.6	78.8	13.6	****
SB1cys-DAH-CM-TM-PMC	14.0	99.8	17.9	##
CM-TM-DMAC	-		>TC*	
G3KLcys-DAH-CM-TM-DMAC	25.8	99.8	16.5	#
G2KLcys-DAH-CM-TM-DMAC	10.3	60	13.2	****
SB1cys-DAH-CM-TM-DMAC	7.9	99	12.4	***

*MIC for conjugates (at physiological pH) is given as µg equivalent of AMPD in the conjugate composition calculated based on the degree of grafting from AAA. *TC: maximal tested concentration*

*of 2000 µg mL^{-1}. Synergy scale: "****" = strong synergy; "***" = synergy; "#" = nearly additive and "##"= slight antagonism*

Biological assays

Antibacterial assay and killing mechanism

To test the antimicrobial activity, the MICs of the chitosan derivatives were measured. The low MICs obtained against Gram-negative *P. aeruginosa* show the high activity of the AMPD coupled with chitosan derivatives (Table 2). In general, all chitosan-AMPDs showed to be active against *P. aeruginosa*, and most of the time we could observe synergistic effects, especially for G3KLcys-DAH-CM-TM-PMC; G2KLcys-DAH-CM-TM-PMC and G2KLcys-DAH-CM-TM-DMAC. G2KLcys coupled with both chitosan derivatives showed higher antimicrobial activity than AMPD alone, most probably due to positive charges coming from CM-TM-PMC or CM-TM-DMAC. In contrast, the parent molecules chitosan, the CM-TM-PMC, and CM-TM-DMAC derivatives had MIC> 2000 µg mL^{-1} at physiological pH, thus showing no measurable antimicrobial activity. This is in agreement with the literature, and it is well known that the antimicrobial activity of the parent chitosan depends on different factors, such as Mw, pH and degree of acetylation/deacetylation.[30]

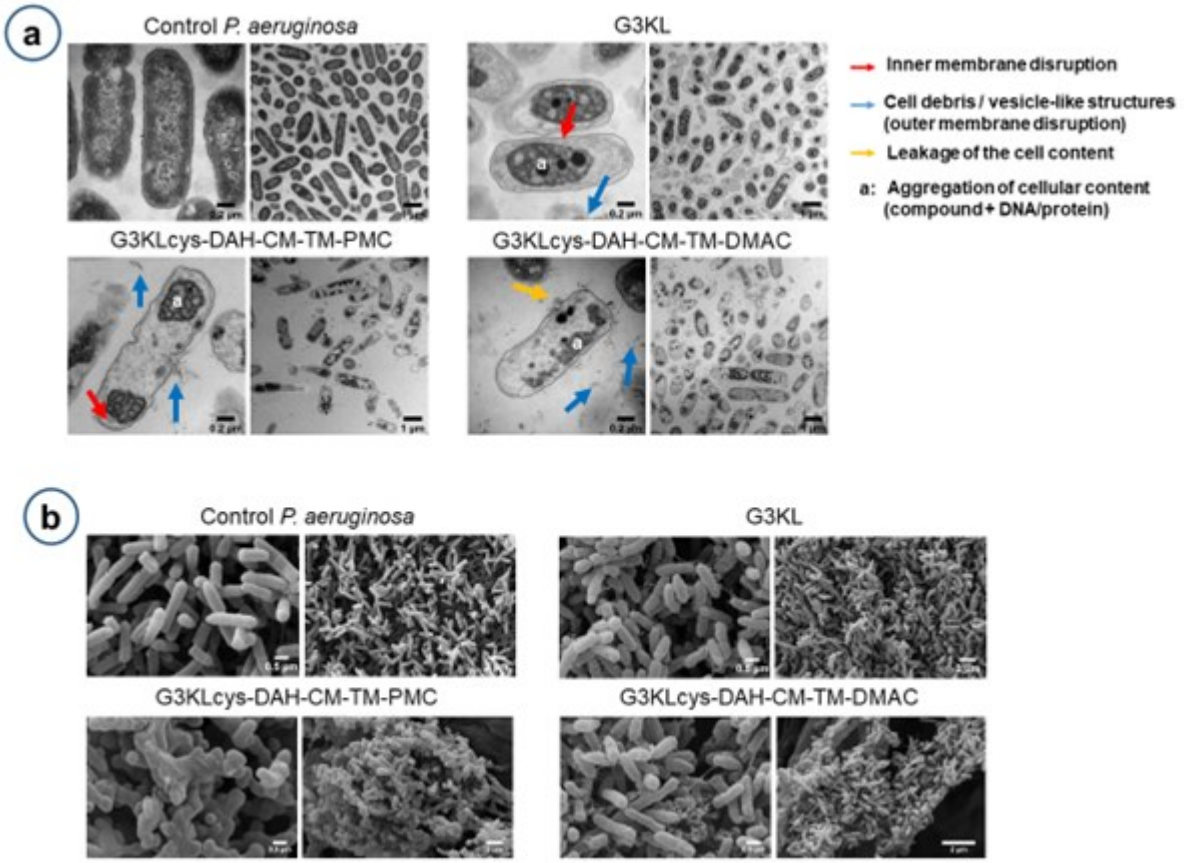

Figure 6. (a) TEM and (b) SEM images for bacteria treated with G3KLcys-chitosan conjugates versus controls: *P. aeruginosa* without treatment and G3KL treated bacteria.

Furthermore, as shown in Table 2, their both DS_{TM} (25%) and DS_{CM} (16% and 22%) are similar. We hypothesize that the charges are compensated due to the presence of additional trimethyl units in TM-DMAC. In addition, the activity of each AMPD-conjugate was highly influenced by the potency of the parent peptide dendrimer. Moreover, the activity is improved upon coupling to chitosan derivatives. We may have expected that the bioactivity of the AMPD/AMP-conjugates would be hindered due to the large size of the peptides and biopolymers. Surprisingly, due to synergistic effects between the compounds, enhanced antibacterial activity was observed upon coupling to chitosan derivatives.

Furthermore, transmission electron microscopy (TEM) images (Figure 6a) show that the bacterial membranes are extensively disrupted, leading to leakage and aggregation of the cellular content. A significant part of the *P. aeruginosa* population was affected when exposed to 2×MIC of AMPD-chitosan conjugates for only 60 min. SEM images (Figure 6b) confirmed morphological changes in the bacterial membrane when treated with both AMPD-chitosan conjugates. Altogether, these results demonstrate that AMPD-chitosan derivatives have similar mechanistic behavior compared to native G3KL, acting by membrane disruption. These data also support the ability of the novel *N*-aryl chitosan derivatives to preserve AMPD activity.

2.2.1 Hemolysis and WST-1 assays

The main limitation of many AMPs is their toxicity towards mammalian cells and lytic activity to RBCs.[24] As such, the safety profile of the new conjugates was further evaluated. The lytic activity of AMPD/AMP chitosan derivatives towards RBCs was tested based on hemolysis assay.

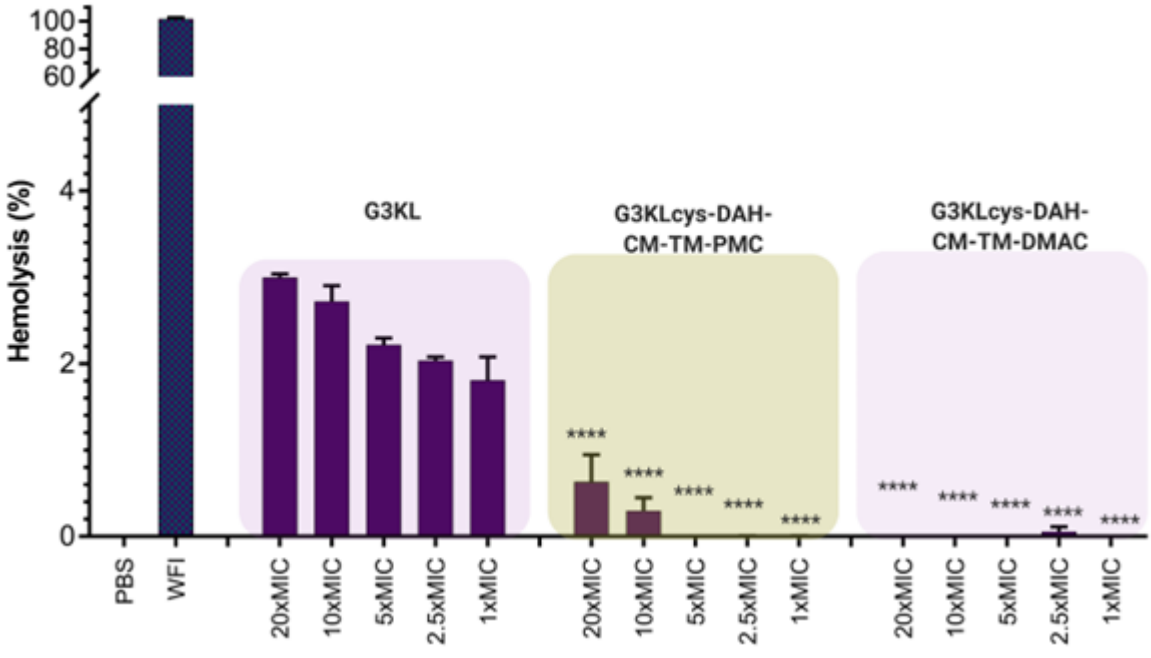

Figure 7. Hemolysis assay for G3KLcys-chitosan conjugates in comparison to native G3KL at the same MIC. The statistics are given for AMPD-conjugates *versus* G3KL at the same concentration. PBS and WFI (water for injection) were used as controls corresponding to 0% and 100% hemolysis, respectively.

As shown in Figure 7, pyridyl derivatives coupled to G3KLcys at 20xMIC were the most hemolytic to RBCs though lysis is as low as 0.9%. This can be expected due to the higher charge density, which also corroborates NMR data. However, it can be considered negligible lysis. Similar results were obtained when coupling G2KLcys or SB1cys to both chitosan derivatives (Figure S19), highlighting that the two molecules showed selective activities to Gram-negative bacteria when chemically linked together while being non-toxic to mammalian cells.

Ş

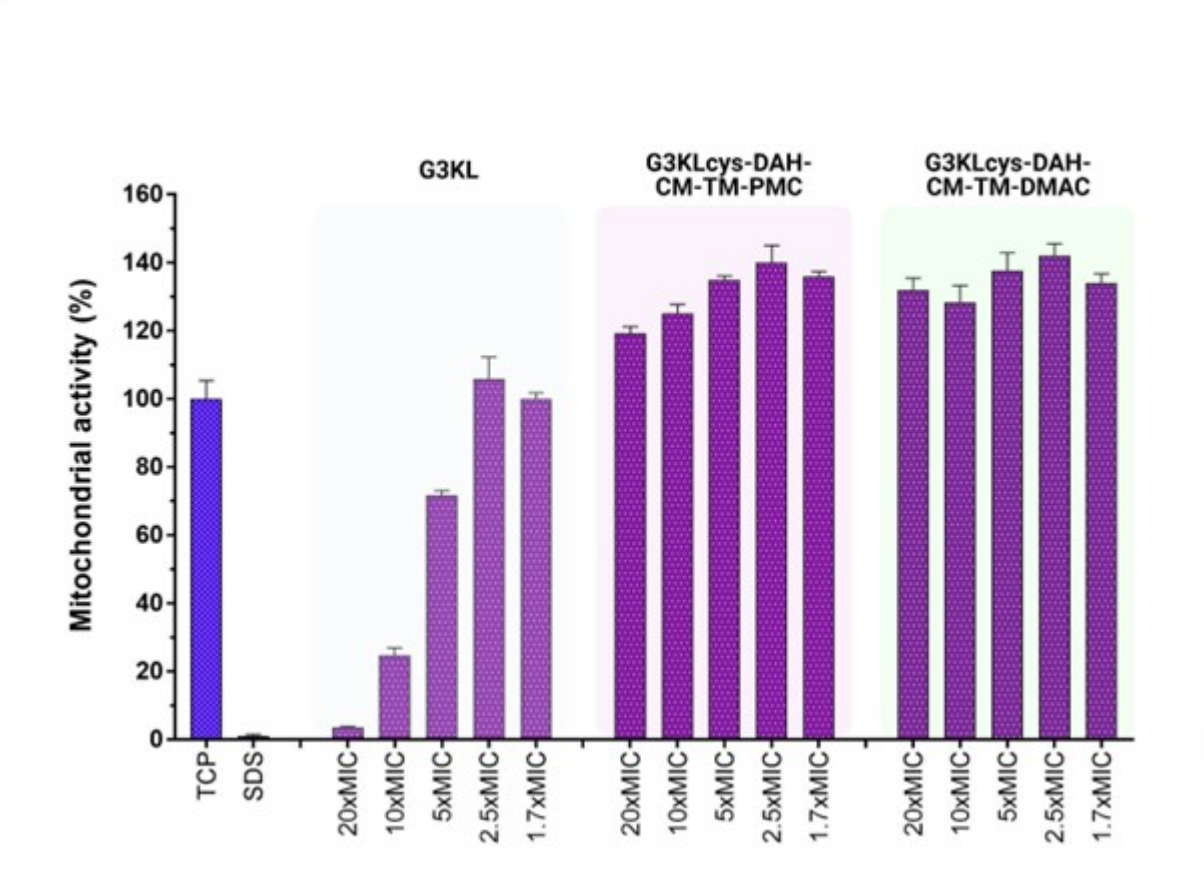

Figure 8. Mitochondrial activity of HDF treated with G3KLcys-chitosan conjugates after 2 days of treatment. The control cells are tissue culture plate (TCP) treated cells and (SDS 1% was used as a positive control).

AMPD-chitosan conjugates had no negative effects on mitochondrial function in HDF cells at all the concentrations evaluated after 48 h of treatment. As shown in Figure 8, the new antimicrobial AMPD-chitosan conjugates exhibit no cytotoxicity to HDF cells even at 20xMIC. Interestingly, the two new conjugates did not show toxicity at 10xMIC and 20xMIC, in contrast to previously developed conjugates based on CMC (*3,6*-di-*O*-carboxymethyl chitosan) (78% viability at 10xMIC, 50% at 20xMIC) and CMTMC (*3,6*-di-*O*-carboxymethyl-*N,N,N*-trimethyl chitosan) (50% viability at 10xMIC and 10% at 20xMIC).[24] This demonstrates a 4-fold increase in the tolerable concentration of the active peptide on fibroblasts. Importantly, the hemolysis levels of the new derivatives remain low, *i.e.,* below 1%, even at 20xMIC concentration. Overall, this in turn improves a key parameter of

antimicrobial active principles, the therapeutic window, *i.e.,* the ratio of effective-to-toxic levels of the active compound, facilitating safe application to patients. Additionally, G2KLcys- and SB1cys-chitosan conjugates exhibited a similar toxicity profile to HDF cells (Figure S20). Therefore, the new antimicrobial conjugates proved to be safe within the tested concentrations ranging from 1x to 20x the MIC.

Overall, both AMPD-chitosan conjugates demonstrated selective properties with a high killing efficacy against *P. aeruginosa* while also being safe for mammalian cells. Moreover, their proof of efficacy must be balanced *against* their cytotoxicity and lysis to blood cells for further clinical applications. In different studies, peptide-polysaccharide conjugates have shown to be promising candidates with different antibacterial activities. *Petrin et al.,* coupled Jelleine-I derived short-chain linear peptide onto a thiolated chitosan backbone using several crosslinkers.[31]. The in vitro investigations on both Gram-positive Staphylococcus aureus and Gram-negative Escherichia coli showed that the chemical coupling strategy resulted in enhanced antibacterial activity when compared to unconjugated peptide and chitosan alone. Additionally, their conjugates were more efficient against *S. aureus* (MIC of 2.8 – 6 μg mL^{-1}) than *E. coli* (MIC of 18 – 24 μg mL^{-1}), and they showed cytotoxicity toward NIH/3T3 fibroblast cells within MIC values for *E. coli*. In a different study, Barbosa et al. used a CuAAC "click-chemistry" reaction *via* azide-alkyne coupling to design an AMP-based material for biomaterials-associated infections.[32, 33] Using Dhvar-5 as an AMP, they have shown low cytotoxicity, further supporting the use of chitosan as an AMP vehicle. Similarly, Sahariah et al. 2015, immobilized anoplin to chitosan with preferential activity against Gram-negative *E. coli* (MIC of 4 μg mL^{-1} of the conjugate or 2.3 μg mL^{-1} corresponding to anoplin) by creating intramolecular and pore-forming clusters of anoplin.[34] Overall, their results show that the activity of the AMP depends on the conjugation strategy, which in turn influences the activity profile of the conjugates. Also, grafting short peptides, like CysHHC10 *via* thiol-maleimide reaction, lead to different bactericidal activity. A higher activity was reported when grafted onto the hydroxyl group of the chitosan than onto the amine.[35] However, the CysHHC10-chitosan conjugate showed only 60% cytocompatibility with fibroblasts. This suggests that the conjugation chemistry of the peptides to polymeric

backbones has to be chemoselective in order to avoid any side effects, like loss of biological activity, cytotoxicity or hemolysis.

Conclusion

This new technology based on chitosan derivatives is an attractive platform for coupling newly developed AMPDs, suitable for coupling not only highly ramified AMPDs (*e.g.,* third generation G3KL) but also for less branched AMPDs, such as second-generation G2KL or even linear AMPs (*e.g.,* SB1). This work highlights the versatility of the chitosan chemistry being efficient for coupling not only linear AMPs but branched ones as well.

The novel antimicrobial agents based on chitosan derivatives CM-TM-PMC and CM-TM-DMAC coupled to G3KLcys exerted strong *in vitro* activities against the opportunistic *P. aeruginosa,* a member of the ESKAPE family. Additionally, we observed high synergistic effects for AMP(D)s upon chemical linking to chitosan derivatives. Furthermore, both chitosan derivatives coupled to G3KL showed safety towards mammalian cells, including HDF and RBCs, which are critical parameters when evaluating the safety profile of a new antimicrobial agent. Moreover, these AMPD conjugates showed improved safety compared to previously published ones based on CMC or CMTMC, allowing their safe use over a broader range of concentrations.

In terms of the mechanism of action, the transmission electron microscopy (TEM) images revealed that AMPD-chitosan conjugates disrupt both the outer and inner membranes of *P. aeruginosa*. This is most likely due to cationic charges coming from the conjugates, as already observed with another conjugate of the same AMPD.

Therefore, the combination of chitosan's antibacterial properties with the potency of the AMPDs could pave the way to develop efficient "antibiotic weapons" against the ESKAPE pathogens. This is a very important breakthrough in the discovery of AMP-biopolymer conjugates against pathogenic bacteria, an urgent unmet need for patients suffering from burns or hard-to-heal wounds (*e.g.,* diabetic or ulcerous wounds). Moreover, the new antibacterial compounds can be further delivered as nanoparticles, bandages, and gels for overcoming AMR infections. The pharmaceutical formulation of the conjugates will benefit from the solubility and the cationic nature of the

derivatives. Nanoparticles can be formed by conventional ionic complexation methods[24] for nebulization or liquid application. The bioactive conjugates can be incorporated in several gels such as those based on hyaluronic acid or collagen, enabling bandage formulation upon lyophilization to overcome wound AMR infections.

Experimental Section

Materials

Experimental Details.

Chitosan (47 kDa; 87% DDA) was a kind gift from Primex (Iceland). *N*-Ethyl-*N*′-(3-dimethyl-aminopropyl)–carbodiimide·HCl (EDC) was purchased from Bachem. 1,6-Diaminohexan (DAH), formaldehyde, *N*-hydroxysuccinimide (NHS), *p*-iodonitrotetrazolium chloride (INT), methyl iodide (CH_3I), 1-methyl-2-pyrrolidone (NMP), *N*-4-pyridine-carboxy-aldehyde, sodium cyanoborohydride ($NaBH_3CN$) and sodium iodide (NaI) was bought from Sigma Aldrich (Switzerland). N-4-dimethylamino-cinnamyl-aldehyde was bought from Merk (Darmstadt, Germany); sulfosuccinimidyl (4-iodoacetyl)aminobenzoate (sulfo-SIAB) – from Brunschwig, Basel, Switzerland; glutaraldehyde - from Agar Scientific, Stansted, Essex, UK; and HEPES was purchased from Fluka, Buchs, Switzerland. All chemicals have been used as received unless mentioned.

Synthesis of *N*-4-pyridylmethyl chitosan (PMC)

PMC derivative was synthesized based on the protocol of Sajomsong et al. with some modifications.[36] Briefly, 1 g of chitosan (6.11 mmol, 1g) was dissolved in 0.2 mol L^{-1} acetic acid (70 mL, *p*H 4.0). The chitosan solution was diluted with 70 mL of ethanol and mixed at room temperature for 1 h. Then, *N*-4-pyridine-carboxyaldehyde (3.055 mmol, 0.33 g) was added to react at 60 °C for 15 h. The pH of the solutions was adjusted to 5.0 using 1 M NaOH. Subsequently, $NaBH_3CN$ (24.46 mmol, 1.54 g) reducing agent was added drop-by-drop to the chitosan solution after being diluted in methanol. The solution was then stirred under reflux conditions for 24 h, followed by a *p*H adjustment to 12. The precipitate was washed, collected, and dissolved in Milli-Q water, followed by 3 days of dialysis (Spectra/Por 4, cut-off 12-14 kDa). The final compound was freeze-dried (yield 80%) and analyzed by FTIR and NMR.

Synthesis of *N*-4-*N*,*N*-dimethylaminocinnamyl chitosan (DMAC)

DMAC derivative was synthesized using the same methodology used for PMC. The 4-*N*, *N*-dimethylaminocinnamaldehyde (3.055 mmol, 0.54 g) was used instead of 4-pyridine-carboxyaldehyde. The final compound was freeze-dried (yield 61%) and analyzed by FTIR and NMR.

Methylation of *N*-aryl derivatives to obtain chitosan TM-PMC (*N*-(4-N,N,N-trimethyl-pyridylmethyl)) and TM-DMAC (*N*-(4-*N*,*N*,*N*-trimethyl-aminocinnamyl))

Methylation of *N*-aryl derivatives was performed following Sajomsang et al.[16] with some modifications. Shortly, 1 g of *N*-aryl derivative (DMAC or PMC) was mixed with 50 mL of NMP for 12 h at room temperature. Then, 8 mL of 15% (w/v) NaOH and 3 g of NaI were added and mixed under reflux at 60 ^{o}C for 15 min. Subsequently, 8 mL of CH_3I was added to the solution in 3 parts at 3 h intervals apart and left to react at 60 ^{o}C for 24 h. The yellow-clear solution was left to cool down at room temperature, followed by precipitation in acetone. The precipitate was then collected and dissolved in 15% (w/v) NaCl and dialyzed for 3 days. Lyophilization of the final products (yields: 64% and 55% for TM-PMC and TM-DMAC, respectively) was run before NMR and FTIR characterization.

Carboxymethylation of TM-PMC and TM-DMAC

The carboxymethylation step followed the methylation step of *N*-aryl chitosan derivatives using the protocols previously reported.[26] TM-PMC or TM-DMAC (1 g) were suspended in 100 mL isopropanol. The solution was mixed overnight at 40 ^{o}C, followed by dropwise addition of 1.5 mL of 50% (w/v) NaOH for 20 min and left to react for an additional 45 min. Next, chloroacetic acid (12.7 mmol, 1.2 g) was added drop-by-drop for 25 min. Then the solution was left to react under reflux and argon atmosphere at 60 ^{o}C for 3 h. The *p*H was adjusted to 7 and then washed with 70% and then pure ethanol. Dialysis was run for 3 days. The final compounds were lyophilized (yield: 48% and 20% for CM-TM-PMC (*3,6*-di-*O*-carboxymethyl-*N*-4-*N,N,N*-trimethyl-pyridylmethyl chitosan) and CM-TM-DMAC (*3,6*-di-*O*-carboxymethyl-*N*-4-*N,N,N*-trimethyl-aminocinnamyl chitosan), respectively) and analyzed by FTIR and NMR.

Addition of 1,6-diaminohexane (DAH) spacer to CM-TM-PMC and CM-TM-DMAC

DAH spacer was attached to chitosan derivatives following previously reported protocols.[27] In brief, synthesized CM-TM-PMC or CM-TM-DMAC (240 mg) were dissolved in TRIS buffer (*p*H 9.0) and left for stirring at elevated temperature. The reaction solution was cooled down before adding 24 mL of each 0.8 mol L^{-1} EDC and 0.2 mol L^{-1} NHS and left to react at 50 °C under reflux for 2 h. To remove any unreacted EDC and NHS, the polymer solution was transferred into an Amicon® ultracentrifugation tube (cut-off 10 kDa) and centrifuged at 4000 rpm at 10 ^{o}C for 2 h. Subsequently, 24 mL of 0.4 mol L^{-1} DAH was added and left to react under reflux at 40 ^{o}C for 2 days. The final compound was dialyzed and lyophilized (yield: 59% and 91% for DAH-CM-TM-PMC and DAH-CM-TM-DMAC, respectively).

AMP & AMPD coupling

Each chitosan derivative, DAH-CM-TM-PMC or DAH-CM-TM-DMAC was solubilized in borate buffer (*p*H=8.2) at a concentration of 1 mg mL^{-1}followed by heating until it reached the boiling point. After cooling down, the reaction mixture, an excess of sulfo-SIAB crosslinker (molar ratio 2:1, 1.7 mg mL^{-1}) was added to each chitosan derivative. The mixture was left to react at 40 ^{o}C in the dark for 1 h. The unreacted crosslinker was removed by purification and washing procedure. Following, AMPDs (G3KLcys, G2KLcys, or SB1cys) were added to the collected precipitate at a molar ratio of 1 to 5. Each AMPD was synthesized and characterized as previously mentioned[24] and prepared in advance in TCEP (3 mg mL^{-1}; 1 mol TCEP to a 1.2 mol AMPD) to avoid any disulfide bridge formation. The sample mixture was left to react in dark at 45 ^{o}C for 7 days followed by filtration and then lyophilization. Amino acid analysis (AAA) was performed to quantify the amount of grafted peptide.

Characterisation methods

NMR measurements

The ^{1}H and ^{13}C, and the 2D ^{1}H-^{13}C Heteronuclear Single Quantum Correlation (HSQC) NMR spectra were performed using a Bruker AV 700 MHz (D_2O and DCl (1%)) spectrometer, with a SampleJet sample charger (Bruker BioSpin, Rheinstetten, Germany). Spectra were treated with MNova software (MestreNova, Santiago de Compostela, Spain).

FTIR spectroscopy

Fourier-transform infrared spectroscopy (FTIR; Tensor 37, Bruker, Germany) was used to identify functional groups in chitosan and its derivatives within the range of 500-4000 cm^{-1} and 64 scans accumulation.

Amino acid analysis (AAA)

The degree of AMPD grafting was evaluated using AAA by vacuum-hydrolysis over 22 h in 6 mol L^{-1} HCl and 0.1% phenol as previously described.[24, 37] Only 40% of the hydrolyzed volume was injected.

Biological assays

Minimal inhibitory concentration (MIC) assay

MIC is defined as the lowest concentration of a compound that will inhibit the growth of a pathogen. The minimal inhibitory concentration (MIC) assay was performed using the standard broth microdilution method.[38]

All polymer stock solutions were prepared at a concentration of 2048 µg mL^{-1} in Muller Hinton Broth (MHB) medium and 100 µL of stock solution was added into the first well of a 96-well microplate followed by serial dilutions. A 100 µL of a bacterial suspension at $7x10^6$ CFU mL^{-1} (colony forming units) was added to each well of the plate. The last two columns were used for control (MHB alone) and for bacterial inoculation with no antimicrobial agent (growth control). Then the samples were incubated at 37 ^oC for 24 h. After incubation, 20 µL of INT (2 mg mL^{-1} in H_2O) was added to each well and the microplates were incubated for another 30 minutes at 37 ^oC. Gentamicin was used as a reference antibiotic with a MIC range of 1 µg mL^{-1} for *P. aeruginosa*. All experiments were performed in triplicates.

Hemolysis assay

The hemolysis assay was performed following the literature[24, 39] with a down-scaling to 50 µL. PBS and water for injection were used as 0 and 100% lysis, respectively. Stock solutions were prepared at an initial concentration of 2048 µg mL^{-1} in phosphate buffer saline (PBS) and diluted by serial successive dilution in PBS in a flat-bottom 96-well microplate. Then, 50 µL of each sample was added to 50 µL RBC solution in a round-bottom microplate and left for stirring (Orbit LS shaker, S2030-LS-B)

at room temperature for 30 min. Following, centrifugation at 4000 rpm was performed. Then 50 µL of the supernatant from each well was separately mixed with 250 µL of pure ethanol into a new microplate and the absorbance was recorded at 412 and 700 nm.

As for the preparation of red blood cells (RBCs), they were obtained from defibrinated sheep blood (SR0051B, Oxoid Ltd. Thermo-Fischer). A 200 µL of sheep blood was added to 1 mL of PBS, very gently mixed, and centrifuged at 1500 rpm for 1-2 minutes. The plasma supernatant was discarded carefully followed by 2 times washing in PBS. The erythrocyte pellets were re-suspended in 11 mL PBS *before* use.

WST-1 assay

The safety of AMPD-conjugates was assessed using WST-1 cellular proliferation reagent (Roche, Switzerland) on human dermal fibroblasts (HDF, human dermal progenitor cells, 12-week male donor, provided by the Regenerative Therapy Unit from the Centre Hospitalier Universitaire Vaudois (CHUV, Lausanne, Switzerland) Ethics Committee Protocol #62/07). Fibroblasts were seeded in a 96-well microplate at $5x10^4$ cells per well and incubated for 48 h at 37 °C and 5% CO_2 atmosphere. Afterwards, DMEM was replaced by polymer solutions dissolved in DMEM (with 10% FBS) at an initial concentration of 2048 µg mL^{-1}. Positive and negative controls were cells treated with DMEM and 1% SDS, respectively. The incubation time with the polymers was 48 h, followed by the addition of 100 µL of WST-1 (dilution 1:10 in DMEM) before reading the absorbance at 450 and 690 nm using a BioTek Microplate Reader (GmbH, Luzern, Switzerland).

Scanning electron microscopy (SEM) with bacteria

P. aeruginosa was grown in LB medium at 37 °C to the mid-logarithmic phase. The samples were prepared as described previously in our protocols and observed by an FEI Technai G2 TEM (80 kV accelerating voltage).[24] All samples were then examined with a scanning electron microscope (Zeiss EVO 40).

Transmission electron microscopy (TEM)

The exponential phase of *P. aeruginosa* PAO1 was adjusted to an OD of 1.0. Following, cells were washed with PBS and treated with native G3KL (40 µg mL^{-1}), G3KLcys-DAH-CM-PMC (40 µg mL^{-1}), or

G3KLcys-DAH-CM-DMAC (40 µg mL^{-1}) in M63 minimal medium (supplemented with 1 mM $MgSO_4$ and 10% glycerol) for 15, 30 and 60 min exposure time. Every time, 1 mL of the bacteria was centrifuged at 12'000 rpm for 3 min and fixed overnight with 2.5% glutaraldehyde in 0.15 mol L^{-1} HEPES following previous protocols.[24]

Statistics

All experimental *in vitro* data were analyzed with GraphPad Prism 6 (GraphPad Software Inc., La Jolla, USA), Two-way ANOVA, and Sidak's multiple comparison tests to assess significance at a level $p < 0.05$. The results are presented as the mean ± standard deviation (n = 3).

Supporting Information

Supporting Information is available from the Wiley Online Library or from the authors.

Acknowledgements

Olivier Jordan and Bee-Ha Gan contributed equally to this work. This work has been supported by the Innogap fund from the Unitec Office of the University of Geneva [No. 1037-A985]. Dr. Viorica Patrulea is a recipient of the Swiss National Science Foundation grant (project ID: P5R5PM_214509). We thank Prof. Lee Ann Applegate (CHUV, Switzerland) for the kind donation of HDF cells. Dr. James Montgomery and the NMR facility (University of Oxford) are acknowledged for running the NMR spectra. Dr. Laurence Marcout is acknowledged for an insightful discussion on NMR spectra treatment. We also thank Analytical Research and Services (University of Bern) for running the AAA. Primex (Iceland) is acknowledged for the kind donation of chitosan. Electron microscopy sample preparation and imaging were performed with devices supported by Mr. Beat Haenni from the Microscopy Imaging Centre of the University of Bern.

Conflict of Interest

The authors declare no conflict of interests.

Received: ((will be filled in by the editorial staff))
Revised: ((will be filled in by the editorial staff))
Published online: ((will be filled in by the editorial staff))

[1] CDC (2019). "Antibiotic Resistance Threats in the United States. Atlanta, GA: U.S. Department of Health and Human Services. https://www.cdc.gov/drugresistance/pdf/threats-report/2019-ar-threats-report-508.pdf, accessed on 4 February 2022."

[2] D. M. P. De Oliveira, B. M. Forde, T. J. Kidd, P. N. A. Harris, M. A. Schembri, S. A. Beatson, D. L. Paterson, M. J. Walker, **2020**, 33(3), e0181-0119.

[3] T. J. Hall, V. M. Villapún, O. Addison, M. A. Webber, M. Lowther, S. E. T. Louth, S. E. Mountcastle, M. Y. Brunet, S. C. Cox, *Biomaterials Science* **2020**, 8(18), 4951-4974.

[4] P. Bowler, C. Murphy, R. Wolcott, *Antimicrobial Resistance & Infection Control* **2020**, 9(1), 162.

[5] P. Prateeksha, V. Sharma, N. Nagpoore, V. Jadaun, C. Rao, B. Singh, *Adv. Funct. Mater.* n/a(n/a), 2214852.

[6] M. R. Gonzalez, V. Ducret, S. Leoni, B. Fleuchot, P. Jafari, W. Raffoul, L. A. Applegate, Y.-A. Que, K. Perron, *Frontiers in Cellular and Infection Microbiology* **2018**, 8(39).

[7] Y. Kawano, O. Jordan, T. Hanawa, G. Borchard, V. Patrulea, *Advances in Wound Care* **2020**, 9(7), 378-395.

[8] B. H. Gan, J. Gaynord, S. M. Rowe, T. Deingruber, D. R. Spring, *Chemical Society Reviews* **2021**, 50(13), 7820-7880.

[9] C. J. L. Murray, K. S. Ikuta, F. Sharara, L. Swetschinski, G. Robles Aguilar, A. Gray, et al., *The Lancet* **2022**, 399(10325), 629-655.

[10] A. J. Kunz Coyne, A. El Ghali, D. Holger, N. Rebold, M. J. Rybak, *Infectious Diseases and Therapy* **2022**, 11(2), 661-682.

[11] R. A. Caires, V. T. da Costa e Silva, E. A. Burdmann, F. O. Coelho, E. C. Costalonga, *Chapter 39 - Drug-Induced Acute Kidney Injury*, Critical Care Nephrology (Third Edition), (C. Ronco, R. Bellomo, J. A. Kellum and Z. Ricci), Elsevier, Philadelphia, **2019**.

[12] T. Cłapa, J. Michalski, A. Syguda, D. Narożna, P. van Oostrum, E. Reimhult, *Research in Microbiology* **2021**, 103817.

[13] N. T. K. Ly, H. Shin, K. C. Gupta, I. K. Kang, W. Yu, *Macromolecular Research* **2019**, 27(5), 504-510.

[14] D. Cui, A. Szarpak, I. Pignot-Paintrand, A. Varrot, T. Boudou, C. Detrembleur, C. Jérôme, C. Picart, R. Auzély-Velty, *Adv. Funct. Mater.* **2010**, 20(19), 3303-3312.

[15] G. Maisetta, A. M. Piras, V. Motta, S. Braccini, D. Mazzantini, F. Chiellini, Y. Zambito, S. Esin, G. Batoni, *Microorganisms* **2021**, 9(5).

[16] W. Sajomsang, P. Gonil, S. Saesoo, *European Polymer Journal* **2009**, 45(8), 2319-2328.

[17] M.-P. Tian, A.-D. Zhang, Y.-X. Yao, X.-G. Chen, Y. Liu, *Carbohydrate Polymers* **2021**, 261117878.

[18] V. Patrulea, G. Borchard, O. Jordan, *Pharmaceutics* **2020**, 12(9), 840.

[19] T. N. Siriwardena, A. Capecchi, B.-H. Gan, X. Jin, R. He, D. Wei, L. Ma, T. Köhler, C. van Delden, S. Javor, J.-L. Reymond, *Angewandte Chemie International Edition* **2018**, 57(28), 8483-8487.

[20] M. Stach, T. N. Siriwardena, T. Köhler, C. van Delden, T. Darbre, J.-L. Reymond, *Angewandte Chemie International Edition* **2014**, 53(47), 12827-12831.

[21] P. Abdel-Sayed, A. Kaeppeli, T. Siriwardena, T. Darbre, K. Perron, P. Jafari, J.-L. Reymond, D. P. Pioletti, L. A. Applegate, *Scientific Reports* **2016**, 6(1), 22020.

[22] F. Ben Jeddou, L. Falconnet, A. Luscher, T. Siriwardena, J.-L. Reymond, C. van Delden, T. Köhler, *Antimicrobial Agents and Chemotherapy* **2020**, 64(4), e02040-02019.

[23] B.-H. Gan, T. N. Siriwardena, S. Javor, T. Darbre, J.-L. Reymond, *ACS Infectious Diseases* **2019**, 5(12), 2164-2173.

[24] V. Patrulea, B.-H. Gan, K. Perron, X. Cai, P. Abdel-Sayed, E. Sublet, V. Ducret, N. P. Nerhot, L. A. Applegate, G. Borchard, J.-L. Reymond, O. Jordan, *Carbohydrate Polymers* **2022**, 280119025.

[25] W. Sajomsang, U. Rungsardthong Ruktanonchai, P. Gonil, O. Nuchuchua, **2009**, 78(4), 945-952.

[26] V. Patrulea, L. A. Applegate, V. Ostafe, O. Jordan, G. Borchard, **2015**, 12246-52.

[27] V. Patrulea, N. Hirt-Burri, A. Jeannerat, L. A. Applegate, V. Ostafe, O. Jordan, G. Borchard, **2016**, 142114-123.

[28] W. Sajomsang, **2010**, 80(3), 631-647.

[29] T.-C. Chou, *Pharmacological Reviews* **2006**, 58(3), 621-681.

[30] M. Másson, *Antimicrobial Properties of Chitosan and Its Derivatives*, Chitosan for Biomaterials III: Structure-Property Relationships, (R. Jayakumar and M. Prabaharan), Springer International Publishing, Cham, **2021**.

[31] T. H. C. Petrin, V. Fadel, D. B. Martins, S. A. Dias, A. Cruz, L. M. Sergio, M. Arcisio-Miranda, M. A. R. B. Castanho, M. P. dos Santos Cabrera, *Biomacromolecules* **2019**, 20(7), 2743-2753.

[32] M. Barbosa, F. Costa, C. Monteiro, F. Duarte, M. C. L. Martins, P. Gomes, *Acta Biomaterialia* **2019**, 84242-256.

[33] M. Barbosa, N. Vale, F. M. T. A. Costa, M. C. L. Martins, P. Gomes, *Carbohydrate Polymers* **2017**, 165384-393.

[34] P. Sahariah, K. K. Sørensen, M. Á. Hjálmarsdóttir, Ó. E. Sigurjónsson, K. J. Jensen, M. Másson, M. B. Thygesen, *Chemical Communications* **2015**, 51(58), 11611-11614.

[35] D. Pranantyo, L. Q. Xu, E.-T. Kang, M. B. Chan-Park, *Biomacromolecules* **2018**, 19(6), 2156-2165.

[36] W. Sajomsang, S. Tantayanon, V. Tangpasuthadol, W. H. Daly, *Carbohydrate Research* **2009**, 344(18), 2502-2511.

[37] S. Kambhampati, J. Li, B. S. Evans, D. K. Allen, *Plant methods* **2019**, 1546-46.

[38] I. Wiegand, K. Hilpert, R. E. Hancock, *Nat. Protoc.* **2008**, 3(2), 163-175.

[39] T. N. Siriwardena, M. Stach, R. He, B.-H. Gan, S. Javor, M. Heitz, L. Ma, X. Cai, P. Chen, D. Wei, H. Li, J. Ma, T. Köhler, C. van Delden, T. Darbre, J.-L. Reymond, *J. Am. Chem. Soc.* **2018**, 140(1), 423-432.

In the context of the search for new antimicrobials, we report herein the synthesis and biological activity of new cationic antimicrobial peptide dendrimers (AMPD) conjugated to chitosan derivatives. These conjugates act as membrane disruptors of *Pseudomonas aeruginosa* by attacking inner and outer bacterial membranes. Besides extremely low toxicity and hemolysis, synergistic properties are obtained upon coupling AMPD to chitosan derivatives.

*Olivier Jordan, Bee-Ha Gan, Sari Alwan, Karl Perron, Emmanuelle Sublet, Verena Ducret, Hua Ye, Gerrit Borchard, Jean-Louis Reymond and Viorica Patrulea**

Highly Potent Cationic Chitosan Derivatives Coupled to Antimicrobial Peptide Dendrimers to Combat *Pseudomonas Aeruginosa*

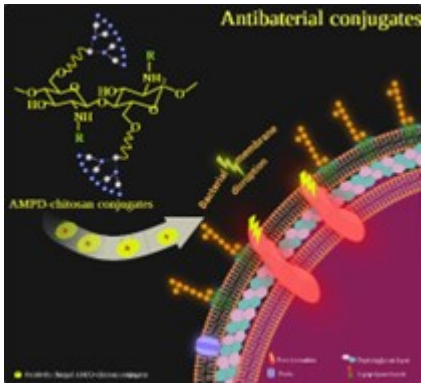

ToC Figure.